Applied Surface Science 323 (2014) 78–81

Contents lists available at ScienceDirect

Applied Surface Science

journal homepage: www.elsevier.com/locate/apsusc

On the origin of anisotropic lithiation in crystalline silicon over germanium: A first principles study

Chia-Yun Chou [a], Gyeong S. Hwang [a,b,*]

[a] Materials Science and Engineering Program, University of Texas at Austin, Austin, TX 78712, USA
[b] Department of Chemical Engineering, University of Texas at Austin, Austin, TX 78712, USA

ARTICLE INFO

Article history:
Received 31 March 2014
Received in revised form 25 August 2014
Accepted 25 August 2014
Available online 2 October 2014

Keywords:
Silicon
Germanium
Crystallographic orientation dependent lithiation
Lithium ion battery anode
Density functional theory

ABSTRACT

Silicon (Si) and germanium (Ge) are both recognized as a promising anode material for high-energy lithium-ion batteries. Si is abundant and best known for its superior gravimetric energy storage capacity, while Ge exhibits faster charge/discharge rates and better capacity retention. Recently, it was discovered that Si lithiation exhibits strong orientation dependence while Ge lithiation proceeds isotropically, although they have the same crystalline structure. To better understand the underlying reasons behind these distinctive differences, we examine and compare the lithiation behaviors at the Li_4Si/*c*-Si(1 1 0) and Li_4Ge/*c*-Ge(1 1 0) model systems using ab initio molecular dynamics simulations. In comparison to lithiated *c*-Si, where a sharp amorphous–crystalline interface remains and advances rather slowly, lithiated *c*-Ge tends to loose its crystallinity rapidly, resulting in a graded lithiation front of fast propagation speed. Analysis of the elastic responses and dynamics of the host Si and Ge lattices clearly demonstrate that from the beginning of the lithiation process, Ge lattice responds with more significant weakening as compared to the rigid Si lattice. Moreover, the more flexible Ge lattice is found to undergo facile atomic rearrangements during lithiation, overshadowing the original crystallographic characteristic. These unique properties of Ge thereby contribute synergistically to the rapid and isotropic lithiation.

1. Introduction

Driven by the increasing demands for lithium-ion batteries (LIBs) with higher energy/power density, there has been a growing interest to replace the current graphite anode with alternative materials of higher Li storage capacities. Among them, silicon (Si) has received tremendous attention because it is abundant and has the highest known theoretical capacity (4200 mAh g^{-1} for $Li_{22}Si_5$ vs. 372 mAh g^{-1} for LiC_6) [1,2]. Germanium (Ge), second only to Si, has a high theoretical capacity of 1624 mAh g^{-1} ($Li_{22}Ge$ [3,4]), but has just begun to draw more research interests, especially in areas where it exhibits superior properties to Si. These include (i) higher intrinsic electrical conductivity [5], (ii) higher room-temperature Li diffusivity, enabling an ultrafast charging rate up to 1000 °C [6], and (iii) more resistive to surface oxidation than Si [7].

Being in the same column in the periodic table, Si and Ge both exist in the tetrahedrally bonded diamond structure with the lattice parameters differ only by 4%. Both are 'alloy-type' anodes, which form amorphous alloys with Li (*a*-Li_xSi/Li_xGe) upon room-temperature lithiation accompanied by large structural/volume changes, leading to early capacity fading [8–11]. Because of these similarities, one might expect Si and Ge to have very similar lithiation/delithiation behavior, but as highlighted by in situ characterizations, Si and Ge appear to have distinctively different responses to electrochemical lithiation/delithiation [12]. For instance, lithiation of crystalline Si (*c*-Si) exhibits a strong orientation-dependence (anisotropic), while crystalline Ge (*c*-Ge) is lithiated isotropically. Furthermore, in comparison to Si, Ge of comparable nano-architecture is able to withstand much faster charging rates with noticeably less crack formation. On the theoretical side, there have been many studies employing density functional theory (DFT) to examine Li incorporation in *c*-Si/*a*-Si bulks and nanowires [13–23] but a few on Ge [24,25]. Nonetheless, the fundamental understanding regarding the nature and origin of their dissimilar responses to lithiation is still limited.

In this paper, on the basis of DFT and ab initio molecular dynamics (AIMD) calculations, we first examine the structural evolution at the lithiation fronts in *c*-Si and *c*-Ge, and it turns out that the two systems are easily distinguished from one another in terms of lithiation mechanism and lithiation propagation speed. To explain the origin of these differences, we investigate the elastic responses

* Corresponding author at: Department of Chemical Engineering, University of Texas at Austin, Austin, TX 78712, USA. Tel.: +1 512 471 4847; fax: +1 512 471 7060.
E-mail address: gshwang@che.utexas.edu (G.S. Hwang).

http://dx.doi.org/10.1016/j.apsusc.2014.08.134
0169-4332/

of Si and Ge lattices upon lithiation as well as the role of their lattice dynamics. The fundamental findings may assist the rational design of the next-generation high performance Si- and Ge-based anodes.

2. Computational methods

Quantum mechanical calculations reported herein were performed on the basis of density functional theory (DFT) within the generalized gradient approximation (GGA-PW91) [26], as implemented in the Vienna Ab-initio Simulation Package (VASP) [27–29]. The projected augmented wave (PAW) method with a plane-wave basis set was used to describe the interaction between core and valence electrons. An energy cutoff of 350 eV was used for geometric optimization of model structures for the a-Li_4Si/Si(1 1 0) and a-Li_4Ge/Ge(1 1 0) interfaces; all atoms were fully relaxed using the conjugate gradient method till residual forces are smaller than 5×10^{-2} eV Å^{-1}. For Brillouin zone sampling, a $(2 \times 2 \times 2)$ k-point mesh was used in the scheme of Monkhorst-Pack [30]; the k-point mesh size should be sufficient considering the disordered nature of the interface systems.

The initial structure for the a-Li_4Si/Si(1 1 0) interface was prepared by stacking an a-Li_4Si bulk model on top of a c-Si supercell in the [1 1 0] direction. The a-Li_4Si model structure consisted of 51 Li and 13 Si atoms has dimensions of 10.914 Å × 11.5761 Å × 8.5576 Å, which were tailored to match the same dimensions of the c-Si lattice in the x and y directions [see Ref. [15] for detailed computational methods]. We used the GGA-optimized lattice constant of 5.457 Å for c-Si, and the 96-atom c-Si supercell has dimensions of 10.914 Å × 11.5761 Å × 15.5761 Å. The a-Li_4Si/Si(1 1 0) system was fully relaxed and then annealed at 500 K for 1 ps to allow sufficient atomic rearrangement, followed by geometry optimization. The a-Li_4Ge/Ge(1 1 0) interface was generated following exactly the same procedures; the a-Li_4Ge model structure consisted of 51 Li and 13 Ge atoms has dimensions of 12.2529 Å × 11.5532 Å × 7.4895 Å, the GGA-optimized Ge lattice constant is 5.777 Å, and the 96-atom c-Ge supercell has dimensions of 12.2529 Å × 11.5532 Å × 23.3557 Å. To simulate the lithiation processes, ab initio molecular dynamics (AIMD) simulations were performed at 1000 K; a time step of 1 fs was used while the temperature was controlled via Nose–Hover thermostat.

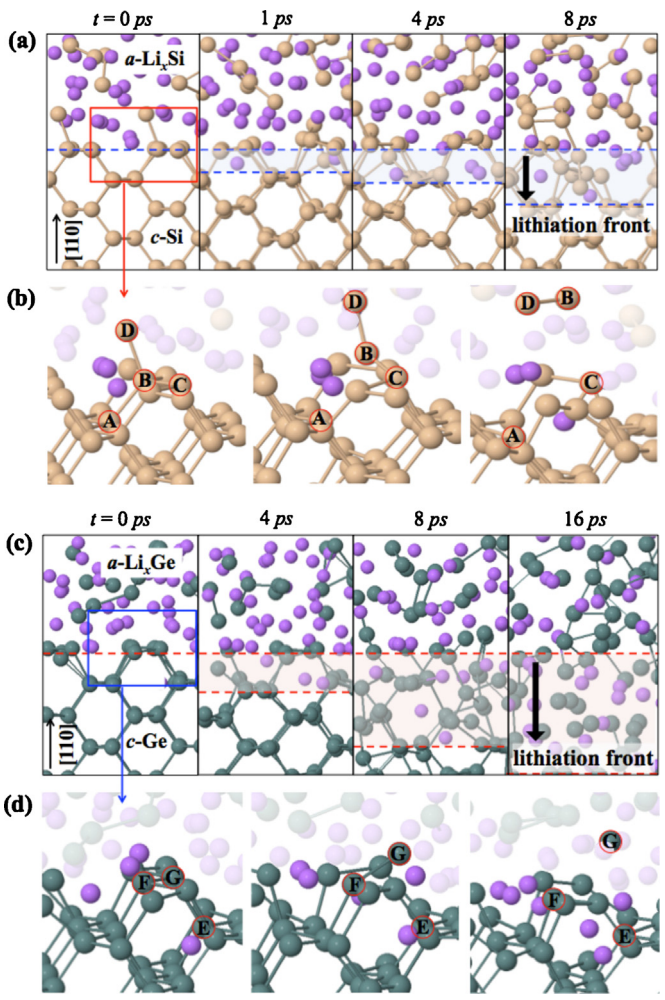

Fig. 1. (a) Structural evolution of the a-Li_4Si/Si(1 1 0) interface with annealing time t = 0, 1, 4 and 8 ps, corresponding to different stages of lithiation. (b) A close up view of interfacial Si atoms break off as dimers (Si_B—Si_D). (c) Structural evolution of the a-Li_4Ge/Ge(1 1 0) interface with annealing time t = 0, 4, 8 and 16 ps. (d) Interfacial Ge atoms mostly break off as monomers (Ge_G).

3. Results and discussion

To examine the anisotropic lithiation behavior of c-Si, the a-Li_4Si/Si(1 1 0) interface was constructed and annealed via AIMD; an annealing temperature of 1000 K was chosen such that the thermal energy is sufficient to agitate atomic movements but far below the melting point of c-Si. The abrupt a-Li_4Si/Si(1 1 0) system can be a realistic representation of the lithiation front considering the following kinetic and energetic points of view. It is now well known that upon lithiation, an a-Li_xSi layer is formed spontaneously at the surface because Li atoms diffuse preferentially along the surface, and driven by the concentration gradient and energetically favorable Li–Si mixing, Li atoms are incorporated into the Si matrix, forming Li_xSi alloys [14,18,19,31]. With the rising Li concentration (x), Li diffusivity (D_{Li}) tends to increase by orders of magnitude [14,15,32], suggesting the solid-state amorphization (converting c-Si into a-Li_xSi alloys) is kinetically feasible at room temperature and such process continues till the most stable alloy composition is reached around x = 4 [15,31]. Given this picture, lithiation of c-Si will be controlled by the reaction at the a-Li_4Si/c-Si interface. Here, only the (1 1 0) crystal orientation is considered since it has been found to be the most favorable facet for Si lithiation [17,25].

Fig. 1(a) shows the structural evolution of the a-Li_4Si/Si(1 1 0) interface with annealing time (t = 0, 4, 8 and 16 ps). During the simulation, the amorphous–crystalline interface (ACI) remains sharp, while Li atoms diffuse into the c-Si region very slowly despite the high annealing temperature. This clearly demonstrates that the lithiation process proceeds in a layer-by-layer fashion, leading to the anisotropic lithiation of c-Si, which is consistent with previous experimental and theoretical findings [17,23]. As Li atoms diffuse into the c-Si region, as shown in Fig. 1(b), the interfacial Si atoms dissolve into the a-Li_4Si region preferentially as dimers (like Si_B—Si_D), apparently due to the weakening of their back bonds (like Si_A—Si_B and Si_B—Si_C) as a result of charge transfer from Li atoms [13,15,17]. In addition, only the interface Si layer is highly distorted whereas the crystallinity in the subinterface layers remains nearly intact, resulting in the sharp ACI.

Next, we examined the lithiation behavior of c-Ge; for direct comparison, the a-Li_4Ge/Ge(1 1 0) interface was constructed and annealed at the same temperature (1000 K). As shown in Fig. 1(c), there appears to be distinct differences between the Ge and Si cases. Compared to the Si case, Li diffusion into the c-Ge region is much faster while the Ge lattice distortion is farther extended beyond the interface layer, resulting in the graded/disordered lithiation front. This suggests that the lithiation of c-Ge may occur isotropically, in contrast to the anisotropically lithiated c-Si, consistent with previous experimental observations [12]. In addition, as Li atoms diffuse into the c-Ge region [Fig. 1(d)], the interfacial Ge atoms break off

Table 1
(a) Calculated bulk modulus (B) of 64-atom c-Si [c-Ge] upon the incorporation of 0, 4 and 9 Li atoms, together with the corresponding degree of host lattice softening. (b) The restoring force acting on a selected c-Si (c-Ge) host atom displaced from its equilibrium position by 0.02 Å in $\pm x$, $\pm y$ and $\pm z$ directions.

(a)	# Li in Si [Ge]	B (GPa)	Softening (%)
	0	88.4 [58.0]	
	4	87.1 [53.2]	1.5 [8.2]
	9	82.1 [46.5]	7.1 [20.0]

(b)	Si (5.457 Å)	Ge (5.777 Å)
Force (eV Å^{-1})	$\begin{bmatrix} -0.13 & 0.00 & 0.00 \\ 0.00 & -0.13 & 0.00 \\ 0.00 & 0.00 & -0.13 \end{bmatrix}$	$\begin{bmatrix} -0.10 & 0.00 & 0.00 \\ 0.00 & -0.10 & 0.00 \\ 0.00 & 0.00 & -0.10 \end{bmatrix}$

and dissolve into the a-Li_4Ge region mostly as monomers (like Ge_C) instead of dimers in the Si case. To better understand the underlying reasons behind the abovementioned differences between c-Si versus c-Ge lithiation, in the following sessions, we analyzed (i) the elastic response and (ii) the dynamic behavior of c-Si and c-Ge lattices upon lithiation.

3.1. Effect of host matrix stiffness

It is well understood that upon lithiation, the transferred charge (from Li) fills the antibonding sp^3 states of neighboring Si (Ge) atoms and thereby weakens the host network [13,15]. Comparisons between Li—Si and Li—Ge bonding interactions and their impacts on a-Li_xSi and a-Li_xGe alloy formation were discussed in our previous work [13,15,24,33]. Here, we will focus on assessing the lithiation-induced softening in c-Si and c-Ge by comparing the variations in the bulk modulus (B) of their 64-atom pristine supercells upon the incorporation of 4 and 9 Li atoms, corresponding to Li concentrations around 6 at.% and 12 at.%, respectively. The geometry and volume of the supercells were re-optimized after the Li incorporation. The B values are determined by fitting the Murnaghan equation of state [34] to the corresponding energy versus volume curve.

$$E(V) = E_0 + \left(\frac{BV}{B'}\right)\left[\frac{(V_0/V)^{B'}}{B'-1} + 1\right] - \frac{V_0 B}{(B'-1)}$$

where E and E_0 refer to the total energies of a given pristine and Li-incorporated c-Si (c-Ge) supercell at volume V and V_0 (equilibrium), respectively; B' is the pressure derivative of B.

In our calculations, uniform tensile and compressive strains were imposed on the systems to achieve ±10% volume variation. As summarized in Table 1(a), the calculated B for c-Si (lattice constant a = 5.457 Å) and c-Ge (a = 5.777 Å) are 88.4 GPa and 58.0 GPa, respectively, in good agreement with the experimental values [35]. As the Li concentration increases to 6 at.% and 12 at.%, B of lithiated c-Si decreases to 87.1 GPa and 82.1 GPa, respectively, showing 1.5% and 7.1% softening. The same trend is observed in lithiated c-Ge, only the reduction in B is much more pronounced (8.2% and 20%), which is reasonable considering that (i) the charge transfer from Li is farther spread in c-Ge [24], corresponding to the more extended lattice softening and (ii) c-Ge of a lower B is likely to be less resistant to the lithiation-induced distortion. According to our analysis, if a Si atom (of the stiffer c-Si lattice) was displaced from its equilibrium position by 0.02 Å in $\pm x$, $\pm y$ and $\pm z$, the restoring force was calculated to be −0.13 eV Å^{-1}; however, if the same condition was applied to a Ge atom (of the less stiff c-Ge lattice), the restoring force was only −0.10 eV Å^{-1} [Table 1(b)]. Therefore, in comparison to Si, Ge shows more appreciable lattice softening upon lithiation, which in turn facilitates faster Li incorporation and amorphization, resulting in the rapid isotropic Ge lithiation.

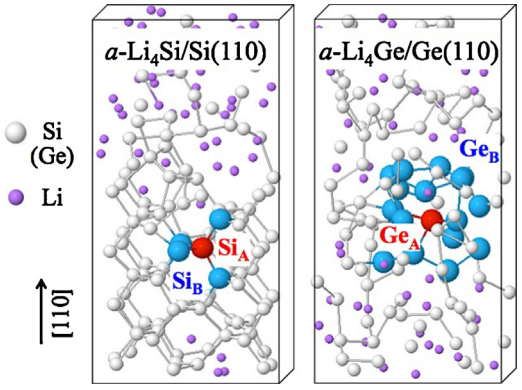

Fig. 2. AIMD snapshots of a-Li_4Si/Si(1 1 0) and a-Li_4Ge/Ge(1 1 0) model systems annealed at 1000 K for 8 ps; the subinterface atom of interest is labeled as 'Si_A' and 'Ge_A' in red color, and the atoms involved in atomic rearrangement during a time interval of 8 ps are marked as 'Si_B' and 'Ge_B' in blue color. (For interpretation of the references to color in this figure legend, the reader is referred to the web version of this article.)

3.2. Role of lattice dynamics

Finally, we examined the dynamic behavior of Si and Ge lattices in the near-interface region as the lithiation front progresses. Fig. 2 shows AIMD snapshots of the a-Li_4Si/Si(1 1 0) and a-Li_4Ge/Ge(1 1 0) systems after 8 annealing at 1000 K. In each system, we randomly selected a Si or Ge atom in a subinterface layer (labeled as 'Si_A' or 'Ge_A' in red color) and tracked its bonded neighbors (marked as 'Si_B' or 'Ge_B' in blue color). The analysis was repeated a sufficient number of times so that the illustration shown here is a good statistical representation. For a time interval of 8 ps, in a-Li_4Si/Si(1 1 0), Si_A tends to remain bonded to the same four Si_B neighbors, suggesting that the subinterface c-Si lattice is nearly stationary and barely rearranges its configuration. This matches the layer-by-layer lithiation mechanism in which only the interface layer is affected by lithiation, yielding the sharp amorphous–crystalline interface (ACI). Contrarily, Ge_A in the a-Li_4Ge/Ge(1 1 0) system is found to undergo migration through a series of bond breaking, bond switching, and new bond forming events. Such facile atomic rearrangements upon lithiation lead to extended lattice disordering far beyond the lithiated layer. As the result, the lithiation front is graded and advances isotropically at a much faster rate as compared to the c-Si case. Likewise, since Ge can easily undergo atomic rearrangements, we also anticipate the matrix to be more flexibly adjusted to the large strain variation during Li insertion/extraction and thereby contribute to the crack reduction and better cycleability.

4. Summary

DFT and AIMD calculations were performed to understand the lithiation behaviors in the a-Li_4Si/Si(1 1 0) and a-Li_4Ge/Ge(1 1 0) model systems; the (1 1 0) crystal orientation is considered since it has been found to be the most favorable facet for Si lithiation. In particular, we examined the structural evolution at the lithiation front, and related which to the distinct elastic response and lattice dynamics pertain to lithiated c-Si and c-Ge. Our simulations show that upon lithiation, c-Si exhibits a sharp amorphous–crystalline interface (ACI), which propagates rather slowly and anisotropically in a layer-by-layer fashion. The weakened Si—Si bonds at ACI break off mostly as dimers and dissolve into the lithiated a-Li_4Si phase. However, lithiated c-Ge exhibits distinctively different lithiation features. As Li atoms diffuse into the c-Ge region, the crystallinity is destroyed rapidly, and the lattice distortion is farther extended beyond the interface layer, resulting in a graded fast-advancing lithiation front. These suggest the lithiation process

proceeds isotropically at a much higher speed in *c*-Ge than *c*-Si. In addition, at the lithiation front, Ge atoms are found to mostly break off as monomers instead of dimers in the Si case. To better understand the underlying reasons behind these differences, we investigated the elastic responses of the *c*-Si and *c*-Ge lattices upon lithiation as well as the role of their lattice dynamics.

Firstly, we found that in comparison to Si, the Ge lattice is more flexible and less resistive to distortion. Upon lithiation, the Li-induced lattice softening is more prominent in Ge. With 4 at.% and 9 at.% Li incorporation, the bulk modulus (B) of *c*-Si is reduced from 88.4 GPa by 1.5% and 7.1%, respectively, while more significant reductions are predicted for lithiated *c*-Ge as B decreases from 58.0 GPa by 8.2% and 20%, respectively. Furthermore, we examined the dynamic behavior of the *c*-Si and *c*-Ge lattices upon lithiation. In comparison to the rather motionless *c*-Si matrix (each Si atom is bonded with the same four nearest neighbors during the entire MD duration), the atomic rearrangements in the Ge lattice tend to extend far beyond the initial adjacent neighbors through a series of bond breaking, bond switching, and new bond forming events.

Our results clearly demonstrate that, with a small degree of Li alloying, the rigid Si lattice responds with less significant weakening as compared to the Ge lattice, thereby well retains the crystallographic properties of unlithiated planes, leading to a sharp amorphous–crystalline interface (ACI) and strong orientation dependence of lithiation. Contrarily, Ge shows pronounced lattice weakening even at low Li concentrations, such that upon lithiation, the original crystallographic characteristic is overshadowed by the sufficiently facile/flexible host atom rearrangements, thereby resulting in the graded lithiation front, which propagates isotropically. Likewise, since Ge can easily undergo atomic rearrangements, the matrix is more flexibly adjusted to the large strain variation during Li insertion/extraction, and thereby minimizes crack formation, leading to improved cycleability. The origin and extended impacts of the anisotropic Si vs. isotropic Ge lithiation are first brought to light in the present work, and we anticipate the improved understanding on the lithiation dynamics may contribute to the design/development of the next-generation high performance Si- and Ge-based anodes.

Acknowledgements

This work was partially supported by the Robert A. Welch foundation (F-1535) and SK Innovation Co., Ltd. We would like to thank the Texas Advanced Computing Center for use of their computing resources.

References

[1] R.A. Sharma, R.N. Seefurth, Thermodynamic properties of the lithium–silicon system, J. Electrochem. Soc. 123 (1976) 1763.
[2] B.A. Boukamp, G.C. Lesh, R.A. Huggins, All-solid lithium electrodes with mixed-conductor matrix, J. Electrochem. Soc. 128 (1981) 725.
[3] C.-M. Park, J.-H. Kim, H. Kim, H.-J. Sohn, Li-alloy based anode materials for Li secondary batteries, J. Chem. Soc. Rev. 39 (2010) 3115.
[4] W.-J. Zhang, A review of the electrochemical performance of alloy anodes for lithium-ion batteries, J. Power Sources 196 (2011) 13.
[5] E.M. Conwell, Properties of silicon and germanium, Proc. Inst. Radio Eng. 40 (1952) 1327.
[6] J. Graetz, C.C. Ahn, R. Yazami, B. Fultz, Nanocrystalline and thin film germanium electrodes with high lithium capacity and high rate capabilities, J. Electrochem. Soc. 151 (2004) A698.
[7] D. Bodlaki, H. Yamamoto, D.H. Waldeck, E. Borguet, Ambient stability of chemically passivated germanium interfaces, Surf. Sci. 543 (2003) 63.
[8] L.Y. Beaulieu, K.W. Eberman, R.L. Turner, L.J. Krause, J.R. Dahn, Colossal reversible volume changes in lithium alloys, Electrochem. Solid State Lett. 4 (2001) A137.
[9] J.H. Ryu, J.W. Kim, Y.E. Sung, S.M. Oh, Failure modes of silicon powder negative electrode in lithium secondary batteries, Electrochem. Solid State Lett. 7 (2004) A306.
[10] Y. Liu, S. Zhang, T. Zhu, Germanium-based electrode materials for lithium-ion batteris, ChemElectroChem 1 (2014) 706.
[11] A. Netz, R.A. Huggins, W. Weppner, The formation and properties of amorphous silicon as negative electrode reactant in lithium systems, J. Power Sources 119–121 (2003) 95.
[12] X.H. Liu, Y. Liu, A. Kushima, S. Zhang, T. Zhu, J. Li, J.Y. Huang, In situ TEM experiments of electrochemical lithiation and delithiation of individual nanostructures, Adv. Energy Mater. 2 (2012) 722.
[13] H. Kim, K.E. Kweon, C.-Y. Chou, J.G. Ekerdt, G.S. Hwang, On the nature and behavior of Li atoms in Si: a first principles study, J. Phys. Chem. C 114 (2010) 17942.
[14] C.-Y. Chou, G.S. Hwang, Surface effects on the structure and lithiation behavior in lithiated silicon: a first principles study, Surf. Sci. 612 (2013) 16.
[15] K. Kim, C.-Y. Chou, J.G. Ekerdt, G.S. Hwang, Structure and properties of Li–Si alloys: a first principles study, J. Phys. Chem. C 115 (2011) 2514.
[16] V.L. Chevrier, J.W. Zwanziger, J.R. Dahn, First principles study of Li–Si crystalline phases: charge transfer, electronic structure, and lattice vibrations, J. Alloys Compd. 496 (2010) 25.
[17] M.K.Y. Chan, C. Wolverton, J.P. Greeley, First principles simulations of the electrochemical lithiation and delithiation of faceted crystalline silicon, J. Am. Chem. Soc. 134 (2012) 14362.
[18] V.L. Chevrier, J.R. Dahn, First principles model of amorphous silicon lithiation, J. Electrochem. Soc. 156 (2009) A454.
[19] V.L. Chevrier, J.R. Dahn, First principles studies of disordered lithiated silicon, J. Electrochem. Soc. 157 (2010) A392.
[20] Q. Zhang, W. Zhang, W. Wan, Y. Cui, E. Wang, Lithium insertion in silicon nanowires: an ab initio study, Nano Lett. 10 (2010) 3243.
[21] T.-L. Chan, J.R. Chelikowsky, Controlling diffusion of lithium in silicon nanostructures, Nano Lett. 10 (2010) 821.
[22] Q. Zhang, Y. Cui, E. Wang, Anisotropic lithium insertion behavior in silicon nanowires: binding energy, diffusion barrier, and strain effect, J. Phys. Chem. C 115 (2011) 9376.
[23] J.W. Wang, Y. He, F. Fan, X.H. Liu, S. Xia, Y. Liu, C.T. Harris, H. Li, J.Y. Huang, S.X. Mao, T. Zhu, Two-phase electrochemical lithiation in amorphous silicon, Nano Lett. 13 (2013) 709.
[24] C.-Y. Chou, H. Kim, G.S. Hwang, A comparative first-principles study of the structure, energetics and properties of Li–M (M = Si, Ge, Sn) alloys, J. Phys. Chem. C 115 (2011) 20018.
[25] M.K.Y. Chan, B.R. Long, A.A. Gewirth, J.P. Greeley, The first-cycle electrochemical lithiation of crystalline Ge: dopant and orientation dependence and comparison with Si, J. Phys. Chem. Lett. 2 (2011) 3092.
[26] P.E. Blöchl, Projector augmented-wave method, Phys. Rev. B 50 (1994) 17953.
[27] G. Kresse, J. Hafner, Ab initio molecular dynamics for liquid metals, J. Phys. Rev. B 47 (1993) 558.
[28] G. Kresse, J. Furthmuller, Efficiency of ab-initio total energy calculations for metals and semiconductors using a plane-wave basis set, Comput. Mater. Sci. 6 (1996) 15.
[29] G. Kresse, J. Furthmuller, Efficient iterative schemes for ab initio total-energy calculations using a plane-wave basis set, J. Phys. Rev. B 54 (1996) 11169.
[30] H.J. Monkhorst, J.D. Pack, Special points for brillouin-zone integrations, Phys. Rev. B 13 (1976) 5188.
[31] P. Limthongkul, Y. Jang, N.J. Dudney, Y.-M. Chiang, Electrochemically-driven solid-state amorphization in lithium–silicon alloys and implications for lithium storage, Acta Mater. 51 (2003) 1103.
[32] Z. Cui, F. Gao, Z. Cui, J. Qu, A second nearest-neighbor embedded atom method interatomic potential for Li–Si alloys, J. Power Sources 207 (2012) 150.
[33] C.-Y. Chou, G.S. Hwang, On the origin of the significant difference in lithiation behavior between silicon and germanium, J. Power Sources 263 (2014) 252.
[34] F.D. Murnaghan, The compressibility of media under extreme pressures, Proc. Natl. Acad. Sci. U. S. A. 30 (1944) 244.
[35] J. Asher, O.C. Jones, J.G. Noyes, G.F. Philips (Eds.), Kaye & Laby's Tables of Physical and Chemical Constants, vol. 45, 16th ed., Longman, Harlow, Essex, 1995, p. 214.